Mineral Inclusions in Sapphire from Basaltic Terranes in Southern Vietnam: Indicator of Formation Model

Doan Thi Anh Vu, Abhisit Salam, Alongkot Fanka, Elena Belousova, and Chakkaphan Sutthirat

Sapphires in southern Vietnam have been discovered in alluvial gem fields derived from Cenozoic basalts. Several syngenetic mineral inclusions were identified by Raman spectroscopy and electron probe microanalysis; they were classified as ferrocolumbite, zircon, alkali feldspar (albite-anorthoclase-oligoclase), pyrochlore, hercynite spinel, and ilmenite (titanohematite series). Geochemical characteristics of these inclusions appear to have evolved from an alkaline felsic suite. Consequently, the original formation of these sapphires would be related to alkaline felsic magmatic processes before basaltic magmatism, which was derived from the deeper upper mantle, had passed through and transported the sapphires and their associated minerals to the surface via volcanic eruption.

Since the late 1980s, sapphire mines in southern Vietnam have supplied significant quantities of gem materials to the jewelry industry (figure 1). Commercial gem mines in southern Vietnam have been located in four main areas, including Dak Nong, Di Linh, Binh Thuan, and Krong Nang (figure 2) (Smith et al., 1995; Long et al., 2004; Garnier et al., 2005; Izokh et al., 2010; Vu, 2010, 2018). Specifically, the first discovery of abundant gem sapphires was in Dak Nong, followed by Di Linh, Binh Thuan, and Krong Nang, respectively. These sapphires accumulated in Upper-Pleistocene to Quaternary alluvial deposits.

In 2017, we carried out field trips in southern Vietnam encompassing Binh Thuan Province, Di Linh (Lam Dong Province), Dak Nong Province, and Krong Nang (Dak Lak Province), where sapphire samples were collected directly from the mines (see figure 2). Gem mining activities in these areas are conducted by a few local miners. Pits are dug with basic tools before washing and hand picking along streams by artisanal miners (figure 3), and mines worked by machinery (figure 4) can also be found. Sapphires in this region usually range from dark blue to bluish green, yellowish green to green, with rare yellow sapphire. The natural intense blue sapphire is the best known and has been specifically recovered from the Dak Nong and Di Linh gem fields (figure 1, left). Other colors such as bluish green and yellowish green to green are common, particularly in the Binh Thuan and Krong Nang gem fields, respectively (figure 1, right). However, these sapphire varieties are generally heat treated for color enhancement. In addition, trapiche-type sapphires (figure 5) are sometimes found in these gem fields.

In Brief

- Several syngenetic mineral inclusions were recognized in sapphires from southern Vietnam.
- Chemical compositions of these mineral inclusions indicated that they evolved from an alkaline felsic suite.
- Alkaline felsic melts were then proposed as the original formation environment of sapphire from basaltic terranes in southern Vietnam.

Gemological properties and chemical fingerprints of sapphire from southern Vietnam have identified this material as basaltic-type (Smith et al., 1995; Long et al., 2004; Garnier et al., 2005; Izokh et al., 2010; Vu, 2010, 2018). However, understanding of their formation remains unresolved. Inclusions in sapphire, including basaltic type, have become a highly interesting issue in the last decade. These inclusions may preserve significant information on chemical and

See end of article for About the Authors and Acknowledgments.
Gems & Gemology, Vol. 56, No. 4, pp. 498–515,
http://dx.doi.org/10.5741/GEMS.56.4.498

Figure 1. High-quality sapphires from southern Vietnam set in rings. Left: The center blue sapphire is approximately 8.8 ct, and the side stones range from 0.3 to 0.4 ct; all are from Di Linh. Right: An approximately 18 ct yellow sapphire from Binh Thuan surrounded by small diamonds. The yellow sapphire was heated to improve its color. Photos by Doan Thi Anh Vu.

physical conditions directly related to the original formation of the basaltic-type sapphire. Subsequently, various analytical techniques such as Raman spectroscopy, scanning electron microscopy

Figure 2. Map of Vietnam showing the distribution of Cenozoic basalts and the main sapphire mining areas in southern Vietnam with the four occurrences where samples were collected (Binh Thuan, Di Linh, Dak Nong, and Krong Nang); modified from Hoa et al. (2005), Lepvrier et al. (2008), Tri and Khuc (2011), and Hoang et al. (2018).

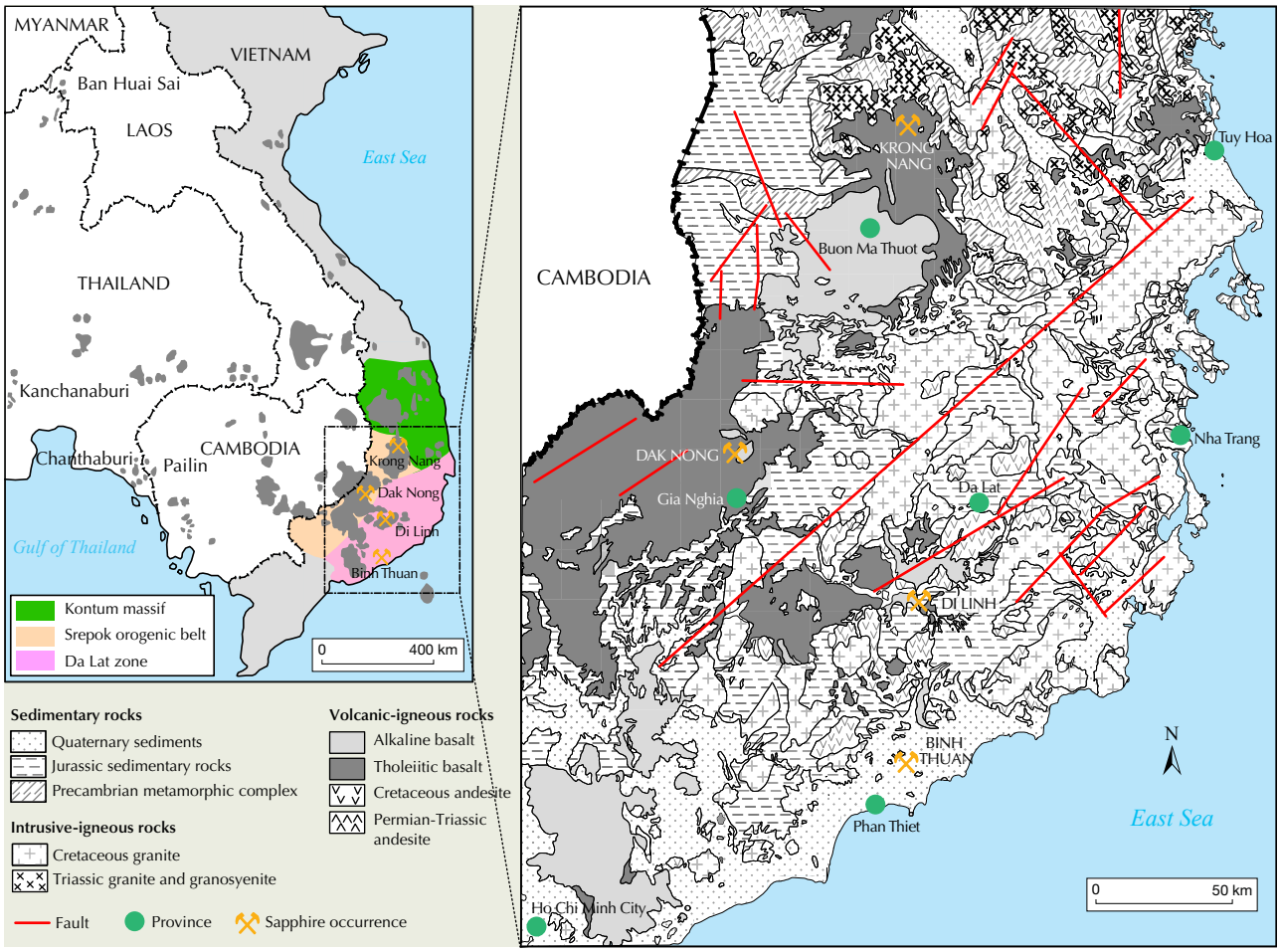

Figure 3. Left: Artisanal miners use crowbars and shovels to remove topsoil and dig through the gem-bearing layer in the Binh Thuan gem field. Right: Gem-bearing gravels are washed and sieved along the stream at Dak Nong. Photos by Doan Thi Anh Vu.

with energy-dispersive spectroscopy (SEM-EDS), and electron probe microanalysis (EPMA) have been applied for identification of inclusions in sapphire from southern Vietnam. For example, Smith et al. (1995) and Long et al. (2004) used SEM-EDS to identify various mineral inclusions in sapphires from Dak Nong and Phan Thiet, whereas Izokh et al. (2010) applied EPMA for chemical analyses of a few inclusions in sapphires from Dak Nong.

Although a variety of mineral inclusions in sapphires from southern Vietnam were previously reported, the chemistry of these inclusions has not been widely analyzed. Therefore, this study is focused on a wider variety of mineral inclusions and

Figure 4. In areas mined with machinery, backhoes were used to remove topsoil and reach the gem-bearing gravel layers prior to washing and sieving using a water pump in the gem fields of Binh Thuan (left) and Krong Nang (right). Photos by Doan Thi Anh Vu.

Figure 5. Trapiche-type sapphires, about 10 ct (left) and 9 ct (right), from Binh Thuan gem field. Photo by Doan Thi Anh Vu.

their chemical analyses using EPMA. These analytical data lead to a reconstruction of a genetic model of sapphire formation related to basaltic volcanism in this region. They also yield significant information for origin determination by gem testing laboratories.

GEOLOGICAL SETTING

Southern Vietnam geologically belongs to a large-scale structure of the Da Lat active continental margin (Da Lat zone) and the Indosinian polyepisodic orogenic belt (Srepok orogenic belt) (figure 2, left) (Tri and Khuc, 2011), which separated from Gondwana in the Devonian (Şengör et al., 1988; Hutchison, 1989; Metcalfe, 1988, 1996, 2009, 2011). Rock formations range widely: Precambrian basement rocks, Jurassic sedimentary rocks, late Mesozoic igneous rocks, and Cenozoic basaltic rocks (Hoa et al., 2005) (figure 2, right). The basement rocks in this area are composed of metamorphic complexes of granulites and gneiss granulite. A thick pile of Jurassic rocks covering the basement rocks is composed of sandstone, siltstone, and shale. These basement rocks and Jurassic rocks are intruded by a number of late Mesozoic rocks, including Triassic granite and granosyenite and Cretaceous granite.

The uppermost part of the area was eventually covered by Cenozoic basalts, which are directly associated with sapphires in southern Vietnam. These Cenozoic (Neogene-Quaternary) basalts range in age from 0.8 to 17.6 Ma (Hoang and Flower, 1998; Garnier et al., 2005) and appear to have been related to the most recent tectonic event, the opening of the East Sea after the Indian-Eurasian collision (from 35 to 17 Ma) (Barr and MacDonald, 1981; Rangin et al., 1995; Hoang and Flower, 1998; Lee et al., 1998). According to Hoang and Flower (1998), these basalts covering an area of about 23,000 km^2 with a thickness of several hundred meters erupted in two main episodes. The early stages mostly included tholeiite basalts, which erupted from extensional fissures trending along the NE-SW and NW-SE directions, derived from the lithosphere. On the other hand, the latter alkali basalts usually flowed along conjugate strike-slip faults originating from the asthenosphere. Only the alkali basalts in particular are associated with sapphire (Smith et al., 1995; Garnier et al., 2005; Izokh et al., 2010). According to Garnier et al. (2005), alkali basalts in Dak Nong are characterized by porphyritic olivine basalts that comprise olivine, clinopyroxene, plagioclase, and spinel. These compositions are associated with megacrysts, xenocrysts, and xenoliths of the mantle and lower crust. Mantle xenoliths embedded in Dak Nong basalts are recognized as garnet lherzolite and spinel lherzolite, while xenocrysts include olivine, Al-rich clinopyroxene, orthopyroxene, phlogopite, sapphire, and zircon. Lower crustal xenoliths usually contain plagioclase and quartz. The presence of mantle xenoliths, xenocrysts, and lower crustal xenoliths may indicate that crystallization of these minerals occurred at high pressure in a magma chamber close to the boundary between the upper mantle and lower crust.

MATERIALS AND METHODS

Over a thousand unheated, gem-quality rough sapphires were collected directly from the gem fields in southern Vietnam (Dak Nong, Di Linh, Krong Nang, and Binh Thuan) for this study. Most of the samples from the Dak Nong and Di Linh mines were collected by the first author over 20 years, while sapphires from Binh Thuan and Krong Nang were collected in 2001 and 2012, respectively. Moreover, more samples from all areas were collected by the authors during the field trip in 2017. These were initially investigated under a gemological microscope to find suitable samples containing mineral inclusions. Subsequently, a total of 274 sapphire samples (77 from Dak Nong, 75 from Di Linh, 45 from Krong Nang, and 77 from Binh Thuan) were then selected and polished to expose the inclusions.

These inclusions were then identified by a Renishaw InVia 1000 laser Raman spectroscope at the Gem and Jewellery Institute of Thailand (Public Organization) (GIT). Subsequently, they were analyzed for major and minor compositions using a JEOL JXA-8100 electron probe microanalyzer at the Depart-

ment of Geology, Faculty of Science, Chulalongkorn University. Operating conditions were set at 15 kV acceleration voltage and 24 nA filament current with 30 seconds of peak and background counts for each element prior to automatic ZAF calculation and reporting in oxide forms. The general detection limits of major and minor analyses obtained from EPMA are typically lower than 0.01 oxide wt.%. Various natural minerals and artificial standards were used for calibration. These included quartz, corundum, eskolaite, fayalite, manganosite, periclase, nickel oxide, wollastonite, jadeite, potassium titanium phosphate, strontium barium niobate, zirconium, yttrium phosphate, cerium phosphate, and neodymium phosphate for SiO_2, Al_2O_3, Cr_2O_3, FeO, MnO, MgO, NiO, CaO, Na_2O, K_2O, Nb_2O_5, ZrO_2, Y_2O_3, Ce_2O_3, and Nd_2O_3, respectively. Fe^{2+} and Fe^{3+} ratios of some specific minerals (e.g., spinel and ilmenite) were estimated by stoichiometric calculation as suggested by Droop (1987). Additionally, a total of four samples that contained zircon inclusions, one from each area, were analyzed for their rare earth elements (REE). These were analyzed using an Agilent 7700 quadrupole ICP-MS instrument, attached to a Photon Machines Excimer 193 nm laser ablation (LA) system at Macquarie University in Sydney, Australia. The analyses were carried out using the same laser conditions as for U-Pb dating. Detailed descriptions of analytical and calibration procedures were given by Belousova et al. (2002). These zircon inclusions were analyzed using a 2 Hz pulse rate with about 0.5 mJ beam energy per pulse, achieving a spatial resolution of about 30 µm. Quantitative results for the trace elements reported here were obtained through calibration of relative element sensitivities using NIST-610 standard glass as the external calibration standard. The BCR-2g and zircon 91500 and GJ-1 reference materials were analyzed within the run as an independent control on reproducibility and instrument stability. Zr content was used for internal calibration for unknown zircon samples (66 wt.% of ZrO_2 as the stoichiometric amount of this oxide in zircon). The precision and accuracy of the NIST-610 analyses were determined to be 1–2% for rare earth elements at the ppm concentration level. Typical detection limits (99% confidence) are provided in table 4.

RESULTS

The most common internal feature of sapphire from southern Vietnam was strong color zoning (figure 6A). Other features included parallel twin planes, needle-like inclusions (figure 6B), liquid-filled inclusions (figure 6C), and negative crystals (figure 6D). Based on Raman spectroscopic and EPMA analyses, 290 mineral inclusions were identified; they were mainly Nb-Ta oxides, followed by silicate and other oxide minerals. The types of mineral inclusions in each sample group are summarized in table 1. Mineral inclusions previously reported in sapphires from Thailand, Laos, and Cambodia are also compared in the same table. Columbite and zircon were the most

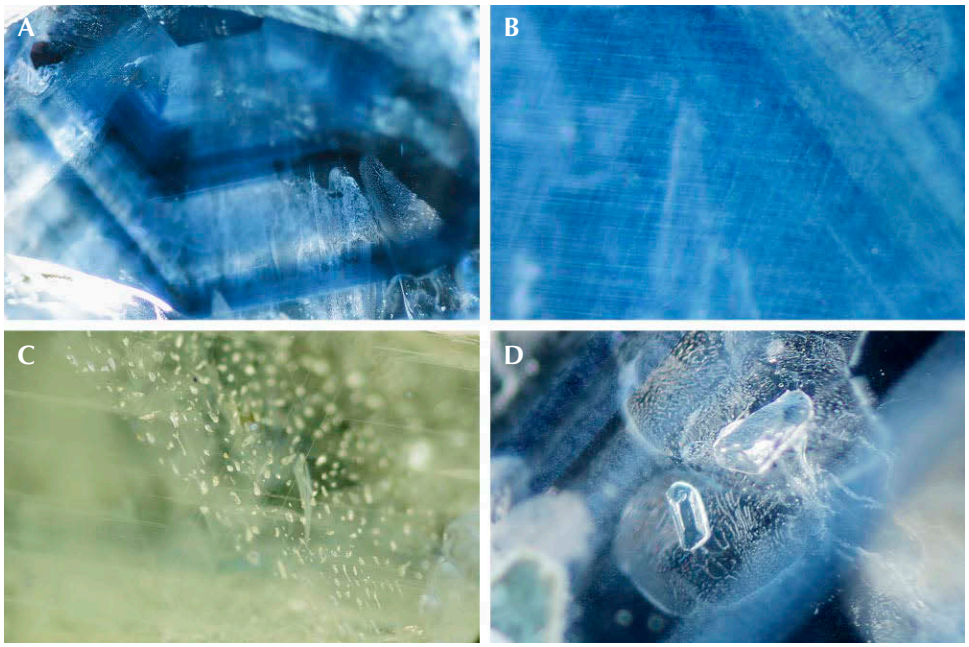

Figure 6. Typical internal features observed in sapphire from southern Vietnam: strong color zones (A), needle-like inclusions (B), liquid-filled inclusions (C), and negative crystals situated in healed fractures (D). Darkfield illumination. Photomicrographs by Doan Thi Anh Vu; magnified 50×.

TABLE 1. Summary of mineral inclusions found in sapphire from southern Vietnam, compared to those reported from basaltic gem fields elsewhere in Southeast Asia.

Area	Nb-Ta oxides	Silicate	Other oxides
Southern Vietnam			
Dak Nong	Columbite*[a] Pyrochlore*	Zircon*[a,b] Alkali feldspar*[a]	Spinel* Ilmenite* Unidentified iron*
Di Linh	Columbite*[c] Pyrochlore[c]	Zircon*[c] Alkali feldspar*[c]	Spinel*[c] Ilmenite[c] Unidentified iron*
Krong Nang	Columbite* Pyrochlore*	Zircon* Alkali feldspar*	Spinel* Unidentified iron*
Binh Thuan	Columbite*[c] Pyrochlore[c]	Zircon*[b,c] Alkali feldspar*[c]	Spinel*[c] Ilmenite[c] Unidentified iron*
Southeast Asia			
Chanthaburi (Thailand)	Columbite[d]	Zircon[d] Alkali feldspar[d]	Spinel[d,e]
Kanchanaburi (Thailand)	–	Zircon[f] Alkali feldspar[f]	Spinel[f] Ilmenite[f]
Ban Huai Sai (Laos)	Columbite[g]	Zircon[e,h] Alkali feldspar[h]	Spinel[e]
Pailin (Cambodia)	Pyrochlore[i]	–	Spinel[g]

**This study, using Raman and EPMA*
[a]Izokh et al. (2010), using EPMA
[b]Long et al. (2004), using SEM-EDS
[c]Smith et al. (1995), using SEM-EDS
[d]Promwongnan and Sutthirat (2019), using Raman and EPMA
[e]Saminpanya and Sutherland (2011), using EPMA
[f]Khamloet et al. (2014), using EPMA
[g]Sutherland et al. (1998b), using EPMA
[h]Sutherland et al. (2002), using EPMA
[i]Palke et al. (2019), using Raman

common inclusions in these sapphire samples, while alkali feldspar and spinel were often identified. Ilmenite, pyrochlore, and unidentified iron minerals were rarely detected. Details of these inclusions are provided below.

Columbite was the predominant mineral inclusion observed in sapphires from all gem fields in southern Vietnam, accounting for nearly 47% of the 290 mineral inclusions contained in the 274 samples. They generally formed as opaque black euhedral crystals with a rhombic prism with pyramidal shape and a truncated rhombic pyramid shape, ranging in sizes from <10 µm up to several millimeters (figure 7, A and B). They were often associated with zircon, with or without feldspar (figures 7C and 9B). Representative EPMA analyses of columbite inclusions

Figure 7. A: A larger prismatic columbite inclusion. B: Two truncated-rhombic columbite inclusions surrounded by healed fractures. C: A cluster of several tiny columbites with colorless feldspar and zircon inclusions. Darkfield illumination. Photomicrographs by Doan Thi Anh Vu; magnified 50×.

TABLE 2. Representative EPMA analyses of columbite inclusions found in sapphires from southern Vietnam, Thailand, and Australia.

Mineral phase analysis (wt.%)	Southern Vietnam								Thailand	Australia	
	Dak Nong		Di Linh		Krong Nang		Binh Thuan		Dak Nong[a]	Chanthaburi[b]	Lava Plains[c]	New England[d]
	DN63	DN68	DL70	DL74	KN25	KN54	PT11	PT73				
TiO_2	2.85	4.06	0.28	1.14	4.78	0.26	nd	12.04	na	0.43	3.57	3.03
FeO	12.32	12.73	15.24	12.35	21.35	15.99	15.96	15.29	15.90	9.79	16.59	17.44
MnO	6.45	6.81	14.64	8.12	0.70	6.55	3.77	4.27	2.93	1.58	2.99	2.19
MgO	0.52	1.38	0.16	2.93	0.77	0.09	nd	0.08	na	0.08	1.18	0.54
CaO	nd	0.05	0.01	0.02	nd	nd	nd	nd	na	0.42	0.03	0.00
Nb_2O_5	75.92	70.02	68.54	72.59	70.80	64.56	76.98	66.03	77.10	74.37	71.98	73.95
Ta_2O_5	0.74	4.45	1.76	1.57	0.50	1.21	3.78	0.46	3.61	0.25	2.98	2.38
ThO_2	nd	0.02	nd	nd	0.02	nd	nd	nd	na	0.85	0.01	na
UO_2	nd	0.08	0.09	nd	0.13	9.97	nd	0.04	na	3.50	0.12	na
ZrO_2	0.41	0.17	0.18	0.26	1.23	0.95	0.03	0.52	0.79	0.78	0.40	0.52
Y_2O_3	nd	nd	nd	nd	nd	0.16	nd	0.15	na	2.76	0.01	na
Nd_2O_3	nd	nd	nd	nd	nd	0.87	nd	nd	na	1.42	na	na
Sm_2O_3	nd	nd	nd	nd	nd	nd	nd	nd	na	0.72	na	na
Total (oxides)	99.2	99.78	100.90	98.98	100.28	100.60	100.53	98.87	100.40	98.61	99.94	100.43
Formula 3(O)												
Ti	0.060	0.086	0.006	0.024	0.099	0.006	–	0.247	–	0.010	0.075	0.064
Fe	0.288	0.299	0.365	0.290	0.494	0.404	0.377	0.348	0.376	0.243	0.388	0.407
Mn	0.152	0.162	0.355	0.193	0.016	0.168	0.090	0.098	0.070	0.040	0.071	0.052
Mg	0.022	0.058	0.007	0.123	0.032	0.004	–	0.003	–	0.004	0.049	0.022
Ca	–	0.002	0.000	0.001	–	–	–	–	–	0.013	0.001	0.000
Nb	0.957	0.888	0.888	0.923	0.886	0.882	0.984	0.813	0.985	0.997	0.909	0.933
Ta	0.006	0.034	0.014	0.012	0.004	0.010	0.029	0.003	0.028	0.002	0.023	0.018
Th	–	0.000	–	–	0.000	–	–	–	–	0.006	0.000	–
U	–	0.001	0.001	–	0.001	0.067	–	0.000	–	0.023	0.001	–
Zr	0.006	0.002	0.002	0.003	0.017	0.014	0.000	0.007	0.011	0.011	0.005	0.007
Y	–	–	–	–	–	0.003	–	0.002	–	0.044	0.000	–
Nd	–	–	–	–	–	0.012	–	–	–	0.019	–	–
Sm	–	–	–	–	–	0.000	–	–	–	0.007	–	–
Total (cations)	1.490	1.538	1.638	1.570	1.549	1.568	1.481	1.522	1.470	1.417	1.521	1.503
Mn/Mn+Fe	0.35	0.35	0.49	0.40	0.03	0.29	0.19	0.22	0.16	0.14	0.15	0.11
Ta/Ta+Nb	0.01	0.04	0.02	0.01	<0.01	0.01	0.33	<0.01	0.03	<0.01	0.02	0.02

Abbreviations: na = not analyzed; nd = not detected
[a]*Izokh et al. (2010)*
[b]*Promwongnan and Sutthirat (2019)*
[c]*Guo et al. (1996)*
[d]*Sutherland et al. (1998a)*

ranged between 65–77 wt.% Nb_2O_5, ≤4.5 wt.% Ta_2O_5, ≤12 wt.% TiO_2, ≤3 wt.% MgO, 12–21 wt.% FeO, and <15 wt.% MnO (table 2); The chemical formula of these columbite inclusions can be expressed as $(Fe_{0.373}Mn_{0.133}Mg_{0.133}Ca_{0.228}Ti_{0.091})(Nb_{0.938}Ta_{0.010}U_{0.001}Zr_{0.007})_2O_6$, which fits very well within the compositional range of ferrocolumbite (figure 8). Their compositions were also equivalent to those previously reported for sapphires from Dak Nong by Izokh et al. (2010) as well as from Lava Plains and New England in Australia (Guo et al., 1996; Sutherland et al., 1998b). Lower FeO contents of columbite inclusions in Bo Welu sapphire

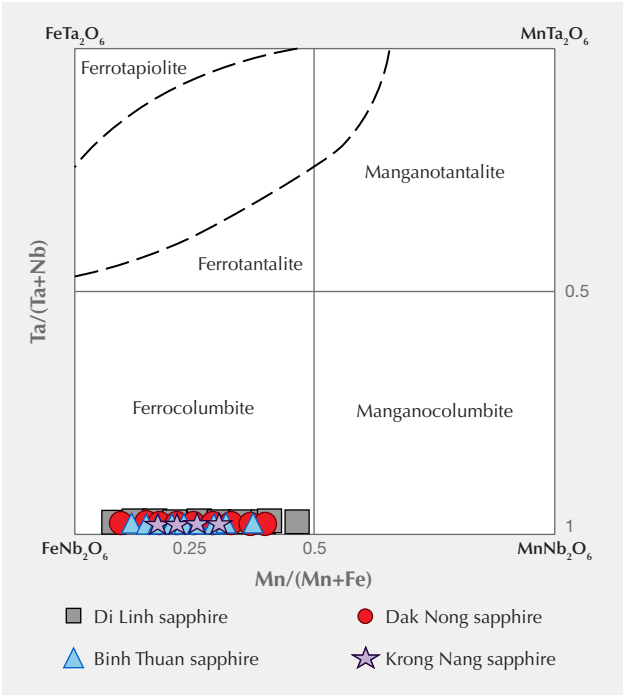

Figure 8. Quadrilateral compositional plots of ferrocolumbite inclusions found in sapphires from southern Vietnam. Various compositional fields and columbite–tapiolite miscibility gap were proposed by Černý and Ercit (1985).

from Chanthaburi, Thailand, were reported by Promwongnan and Sutthirat (2019). Ferrocolumbite inclusions in sapphire from southern Vietnam contained low Ta content, yielding a Ta/(Ta+Nb) ratio < 0.05 within a wide range of Mn contents (<15 wt.% MnO and Mn/(Mn+Fe) ratio <0.5) (figure 8), which may have derived from peralkaline complexes (peralkaline granite/syenite) (Mackay and Simandl, 2015).

Zircon was the second most abundant inclusion, representing about 22% of the mineral inclusions contained in the sapphire samples. These inclusions commonly formed as euhedral tetragonal prismatic or dipyramidal crystals (figure 9, A and B). Most of the zircons were colorless, but some had orange to orange-red colors. Their chemical compositions varied within narrow ranges of approximately 31–34 wt.% SiO_2 and 61–65 wt.% ZrO_2 (table 3). The hafnium contents showed a slightly wider range of about 1–4 wt.%, leading to Hf/Zr ratios of 0.01 to 0.04, which fall in the range of magmatic zircon, particularly syenite and granite zircons (Deer et al., 2013). Significant trace elements included <1.5 wt.% ThO_2, <1.8 wt.% UO_2, and <0.6 wt.% Y_2O_3; these elements appeared to be higher in zircon inclusions of Di Linh sapphire. On the other hand, these zircon inclusions yielded Th/U ratios >0.2, indicating a magmatic source (Williams and Claesson, 1987; Rubatto and Gebauer, 2000; Huong et al., 2016). These were similar in composition to zircon analyses previously reported from Dak Nong (Izokh et al., 2010) and other basalt-associated sources such as Ban Huai Sai in Laos, Kanchanaburi in Thailand, and Kings Plains and New England in Australia (Guo et al., 1996; Sutherland et al., 1998a; 2002; Khamloet et al., 2014), although the Y_2O_3 content of zircon inclusions from Bo Welu in Thailand (Promwongnan and Sutthirat, 2019) has recently been reported with a higher content. Total REE contents of representative zircon inclusions ranged from 1156 to 2710 ppm (table 4), more similar to those from syenite pegmatite (2043 ppm) and granitoid (1813 ppm) than those from carbonatite (600–700 ppm) (Belousova et al., 2002).

Alkali feldspar inclusions were sometimes observed in the sapphire samples, making up about 13% of the mineral inclusions. They generally presented subhedral or euhedral grains with small sizes ranging from about 40 µm, with some rare examples reaching 1 mm. These included crystals were commonly transparent and colorless (figures 7C and 9C).

Figure 9. A: Prismatic orange zircon inclusion. B: Colorless dipyramidal zircon inclusion surrounded by radial cracks, associated with black columbite inclusions. C: Tiny euhedral feldspar inclusions. Darkfield illumination. Photomicrographs by Doan Thi Anh Vu; magnified 50×.

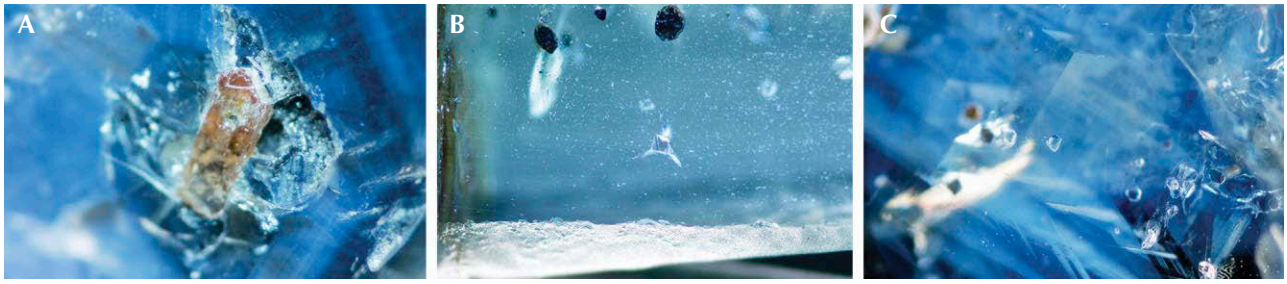

TABLE 3. Representative EPMA analyses of zircon inclusions found in sapphires from southern Vietnam, Laos, Thailand, and Australia.

Mineral phase analysis (wt.%)	Southern Vietnam									Laos	Thailand		Australia	
	Dak Nong		Di Linh		Krong Nang		Binh Thuan		Dak Nong[a]	Ban Huai Sai[b]	Chantha-buri[c]	Kancha-naburi[d]	Kings Plains[e]	New England[f]
	DN23	DN31	DL18	DL44	KN15	KN13	PT36	PT65						
SiO_2	32.16	32.43	34.34	32.59	33.84	33.43	31.19	33.86	32.34	31.23	33.63	34.14	32.12	31.48
TiO_2	0.03	0.02	nd	0.01	0.01	nd	0.06	nd	na	na	na	na	<0.01	0.00
Al_2O_3	0.27	0.30	nd	nd	nd	nd	0.28	0.01	na	0.01	0.01	0.17	0.02	0.44
FeO	nd	0.02	0.04	nd	nd	0.10	0.31	nd	na	na	0.07	0.04	0.20	0.13
MgO	0.02	0.01	nd	nd	nd	nd	0.02	0.01	na	0.01	na	na	<0.01	0.00
CaO	0.06	0.05	nd	nd	nd	0.01	0.01	nd	na	na	na	0.00	0.02	0.00
Na_2O	nd	nd	nd	nd	nd	nd	0.04	nd	na	na	na	na	na	0.00
K_2O	0.02	nd	nd	nd	nd	0.05	0.67	nd	na	na	na	na	na	0.00
ThO_2	0.03	0.31	0.11	1.40	0.32	0.03	0.13	0.09	0.76	0.18	1.21	na	0.49	0.11
UO_2	0.12	1.40	0.12	1.73	0.23	0.06	0.17	0.34	0.93	0.41	1.13	na	0.84	0.11
ZrO_2	64.47	61.44	62.20	61.00	63.98	63.29	63.78	62.02	63.96	64.02	59.39	62.40	63.78	64.84
HfO_2	1.62	3.70	2.51	3.08	2.00	2.82	2.62	3.85	2.44	3.58	2.62	3.50	2.88	2.58
P_2O_5	0.13	0.16	nd	0.22	0.08	0.09	0.32	0.23	na	0.25	0.57	na	0.34	na
Y_2O_3	0.02	0.08	0.27	0.56	0.05	0.07	0.28	0.03	na	0.80	0.85	na	0.34	0.46
Total (oxides)	98.93	99.91	99.60	100.58	100.52	99.96	99.87	100.42	100.43	100.55	99.57	100.25	101.04	100.15
Formula 4(O)														
Si	0.996	1.008	1.048	1.013	1.028	1.024	0.971	1.033	1.001	0.973	1.035	1.036	0.989	0.976
Ti	0.001	0.000	–	0.000	0.000	–	0.001	–	–	–	–	–	–	0.000
Al	0.010	0.011	–	–	–	–	0.010	0.000	–	0.000	0.000	0.006	0.001	0.016
Fe	–	0.000	0.001	–	–	0.003	0.008	–	–	–	0.002	0.001	0.046	0.003
Mg	0.001	0.001	–	–	–	–	0.001	0.000	–	0.000	–	–	–	0.000
Ca	0.002	0.002	–	–	–	0.000	0.000	–	–	–	–	0.000	0.001	0.000
Na	–	–	–	–	–	–	0.003	–	–	–	–	–	–	0.000
K	0.001	–	–	–	–	0.002	0.027	–	–	–	–	–	–	0.000
Th	0.000	0.002	0.001	0.010	0.002	0.000	0.001	0.001	0.005	0.001	0.008	–	0.003	0.001
U	0.001	0.010	0.001	0.012	0.002	0.000	0.001	0.002	0.006	0.003	0.008	–	0.006	0.001
Zr	0.974	0.931	0.925	0.924	0.948	0.945	0.968	0.923	0.965	0.972	0.891	0.923	0.957	0.980
Hf	0.014	0.033	0.022	0.027	0.017	0.025	0.023	0.033	0.022	0.032	0.023	0.036	0.025	0.023
P	0.003	0.004	–	0.006	0.002	0.002	0.008	0.006	–	0.007	0.013	–	0.009	–
Y	0.000	0.001	0.004	0.009	0.001	0.001	0.005	0.000	–	0.013	0.014	–	0.006	0.008
Total (cations)	2.004	2.003	2.002	2.001	2.000	2.003	2.028	1.999	2.000	2.002	1.995	2.002	2.001	2.008
Th/U	0.29	0.23	0.93	0.83	1.42	0.51	0.79	0.26	0.84	0.45	1.10	–	0.60	1.02
Hf/Zr	0.02	0.04	0.02	0.03	0.02	0.03	0.02	0.04	0.02	0.03	0.03	0.03	0.03	0.02

Abbreviations: na = not analyzed; nd = not detected
[a]*Izokh et al. (2010)*
[b]*Sutherland et al. (2002)*
[c]*Promwongnan and Sutthirat (2019)*
[d]*Khamloet et al. (2014)*
[e]*Guo et al. (1996)*
[f]*Sutherland et al. (1998a)*

Their chemical compositions were rather uniformly toward Na-rich feldspar between albite-anorthoclase-oligoclase ($Ab_{77–98}An_{<15}Or_{1–11}$, see table 5 and figure 10). However, feldspar in Krong Nang sapphires mostly plotted close to the junction of albite-anorthoclase-oligoclase compositions ($Ab_{82–86}An_{6–11}Or_{6–11}$),

TABLE 4. REE analyses (ppm) of representative zircons found in southern Vietnam sapphire, determined by LA-ICP-MS.

Element	Dak Nong	Di Linh	Krong Nang	Binh Thuan	Typical detection limits (99% confidence)
	DN05	DL46	KN08	PT05	
Y	1468.21	4220.35	1194.74	2868.13	0.004
La	0.02	nd	0.01	nd	0.004
Ce	2.79	12.00	1.65	13.33	0.003
Pr	0.01	0.06	0.02	0.0523	0.003
Nd	0.27	1.11	0.26	1.451	0.014
Sm	1.23	5.62	0.68	5.62	0.019
Eu	0.96	5.12	0.59	2.177	0.006
Gd	12.91	54.66	5.74	44.06	0.019
Tb	7.23	27.58	3.91	21.66	0.003
Dy	122.00	416.17	76.25	310.13	0.013
Ho	50.02	152.71	38.25	104.29	0.003
Er	258.30	672.98	258.42	442.14	0.009
Tm	60.40	134.11	83.73	89.21	0.003
Yb	566.33	115.50	1081.3	721.34	0.018
Lu	80.77	140.18	179.34	81.68	0.003
Total REE	1155.94	2710.22	1762.23	1815.47	

Abbreviation: nd = not detected

whereas Di Linh feldspar was divided into two groups: the first group close to the albite-anorthoclase boundary ($Ab_{82–85}An_{6–9}Or_{8–11}$) and the second one containing lower K content near the albite-oligoclase boundary ($Ab_{85–87}An_{7–11}Or_{4–5}$). Binh Thuan feldspar ranged between albite and oligoclase compositions, while most Dak Nong feldspar fell within albite composition ($Ab_{83–98}An_{1–10}Or_{1–8}$). These compositional ranges were wider than those previously reported, as only oligoclase was identified in sapphires from Dak Nong (Izokh et al., 2010) and from Ban Huai Sai in Laos (Sutherland et al., 2002), but An and Or components were narrower in range than those in Thai sapphires from Kanchanaburi ($An_{9–23}Or_{6–14}$) (Khamloet et al., 2014) and Chanthaburi ($An_{<14}Or_{7–17}$) (Promwongnan and Sutthirat, 2019) and Australian sapphires from Kings Plains ($An_{<14}Or_{7–17}$)

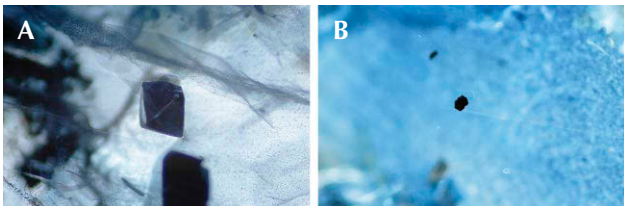

Figure 11. Inclusions of black octahedral hercynite spinel (A) and euhedral rhombohedral ilmenite (B). Darkfield illumination. Photomicrographs by Doan Thi Anh Vu; magnified 50×.

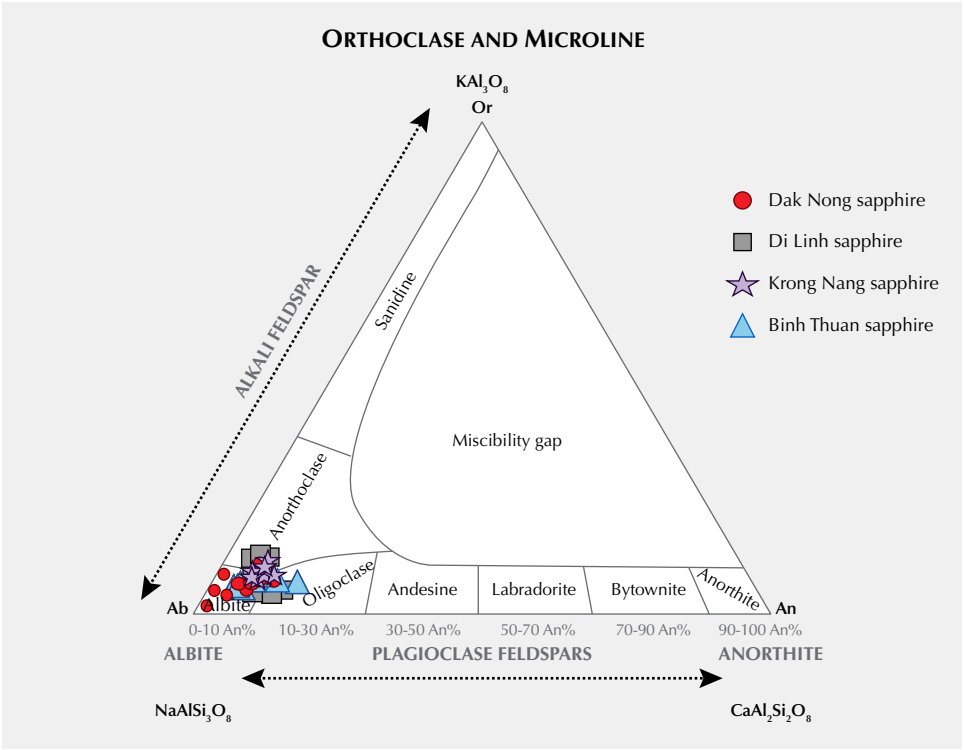

Figure 10. Ternary plot of An-Ab-Or in alkali feldspar inclusions in sapphires from southern Vietnam. Modified from N.N. Greenwood and A. Earnshaw, Chemistry of Elements *(1998), p. 357.*

TABLE 5. Representative EPMA analyses of feldspar inclusions in sapphires from southern Vietnam, Laos, Thailand, and Australia.

Mineral phase analysis (wt.%)	Southern Vietnam								Laos	Thailand		Australia	
	Dak Nong		Di Linh		Krong Nang		Binh Thuan		Dak Nong[a]	Ban Huai Sai[b]	Kanchanaburi[c]	Chanthaburi[d]	Kings Plains[e]	New England[f]
	DN41	DN34	DL27	DL34	KN53	KN37	PT01	PT23						
SiO_2	67.93	64.13	65.66	62.30	65.83	64.38	68.89	64.31	64.20	64.83	65.60	66.97	64.81	53.47
TiO_2	0.02	nd	0.01	0.02	0.01	0.01	nd	nd	0.00	na	0.01	0.02	na	0.00
Al_2O_3	19.06	21.92	23.72	23.73	22.86	21.79	19.70	22.39	22.10	21.45	21.50	21.40	18.56	29.28
FeO	0.03	0.06	0.03	0.19	0.09	0.07	nd	0.06	0.06	0.03	0.04	0.65	na	0.09
MnO	nd	nd	nd	nd	nd	nd	nd	nd	0.02	na	0.00	0.04	na	0.00
MgO	nd	nd	nd	nd	nd	nd	nd	nd	0.00	na	0.05	nd	na	0.00
BaO	0.07	0.01	0.03	0.06	0.07	nd	0.02	0.03	na	na	na	na	na	na
CaO	0.17	2.24	1.09	1.64	1.54	2.24	nd	2.98	3.13	1.96	2.59	0.73	<0.01	11.19
Na_2O	11.33	9.65	7.63	10.76	8.73	9.22	11.37	9.02	9.71	9.37	4.31	2.69	0.73	5.50
K_2O	0.22	1.15	1.60	1.02	1.70	1.44	0.32	1.43	0.82	1.53	6.52	8.47	15.50	0.48
Total (oxides)	98.83	99.16	99.76	99.72	100.84	99.15	100.31	100.22	100.10	99.17	100.62	100.97	99.60	100.01
Formula 8(O)														
Si	3.003	2.857	2.872	2.775	2.872	2.868	2.998	2.841	2.840	2.885	2.908	2.957	2.997	2.425
Ti	0.001	–	0.000	0.001	0.000	0.000	–	–	–	–	0.000	0.001	–	–
Al	0.993	1.151	1.223	1.245	1.175	1.144	1.010	1.166	1.152	1.125	1.124	1.114	1.011	1.565
Fe	0.001	0.002	0.001	0.007	0.003	0.003	–	0.002	0.002	0.001	0.002	0.024	–	0.003
Mn	–	–	–	–	–	–	–	–	0.001	–	–	0.001	–	–
Mg	–	–	–	–	–	–	–	–	–	–	0.003	0.000	–	–
Ba	0.001	0.000	0.000	0.001	0.001	–	0.000	0.001	–	–	–	0.000	–	–
Ca	0.008	0.107	0.051	0.078	0.072	0.107	–	0.141	0.148	0.093	0.123	0.035	–	0.544
Na	0.971	0.833	0.647	0.929	0.738	0.796	0.959	0.772	0.833	0.808	0.371	0.230	0.065	0.484
K	0.012	0.065	0.089	0.058	0.095	0.082	0.018	0.081	0.046	0.087	0.369	0.477	0.914	0.028
Total (cations)	4.991	5.016	4.884	5.095	4.957	4.999	4.986	5.003	5.023	5.000	4.899	4.893	4.988	5.048
Atomic (%)														
Albite	97.9	82.9	82.1	87.2	81.6	80.8	98.2	77.7	81.1	81.8	43.0	31.0	6.7	45.8
Anorthite	0.8	10.6	6.5	7.4	8.0	10.9	0.0	14.2	14.4	9.5	14.2	4.7	0.0	51.5
Orthoclase	1.3	6.5	11.3	5.4	10.5	8.3	1.8	8.1	4.5	8.8	42.8	64.3	93.3	2.7

Abbreviations: na = not analyzed; nd = not detected
[a]*Izokh et al. (2010)*
[b]*Sutherland et al. (2002)*
[c]*Khamloet et al. (2014)*
[d]*Promwongnan and Sutthirat (2019)*
[e]*Guo et al. (1996)*
[f]*Sutherland et al. (1998a)*

(Guo et al., 1996) and New England ($An_{<53}Or_{22–94}$) (Sutherland et al., 1998a).

Spinel inclusions accounted for about 4% of the mineral inclusions contained in the samples from southern Vietnam. They usually occurred as black cubic crystals (figure 11A). Spinel inclusions with compositions ranging between chromite-hercynite and magnetite-hercynite have been previously reported, on the basis of SEM-EDS analyses, in sapphires from Binh Thuan and Di Linh (Smith et al., 1995). However, EPMA analyses of spinel inclusions in this study revealed significant components of hercynite ($FeAl_2O_4$, $Hc_{78–100}$) and spinel ($MgAl_2O_4$, $Sp_{<23}$), whereas other components were negligible (table 6). The spinel inclusions' $Mg:Fe^{2+}$ ratios were mostly less than 1:4, falling into hercynite spinel (Deer et al., 2013). In comparison, these hercynite spinel inclusions contained a moderately lower spinel composition than those in

TABLE 6. Representative EPMA analyses of spinel inclusions in sapphires from southern Vietnam, Thailand, Cambodia, and Australia.

Mineral phase analysis (wt.%)	Southern Vietnam							Thailand	Cambodia	Australia
	Dak Nong		Di Linh	Krong Nang		Binh Thuan		Kanchanaburi[a]	Pailin[b]	New England[c]
	DN12	DN16	DL62	KN42	KN47	PT22	PT34			
SiO_2	nd	nd	0.01	nd	nd	nd	0.25	0.03	0.03	0.00
TiO_2	0.12	0.08	0.70	0.13	0.18	nd	1.91	0.07	0.26	0.13
Al_2O_3	60.99	60.93	60.76	60.31	60.11	61.18	61.58	59.52	63.00	57.04
Cr_2O_3	nd	nd	0.09	nd	nd	nd	nd	0.16	0.29	0.00
FeO_{total}	33.99	34.18	33.87	34.96	33.77	33.35	35.53	35.39	21.77	34.66
MnO	nd	0.89	0.34	0.05	1.18	0.53	1.44	0.22	0.15	0.48
MgO	4.02	4.29	4.62	3.17	4.31	4.60	0.08	5.85	13.50	6.09
ZnO	0.12	0.38	0.18	nd	0.51	0.93	0.07	0.14	na	0.69
CaO	0.06	nd	nd	nd	nd	nd	nd	0.00	<0.005	0.00
Total (oxides)	99.29	100.74	100.58	98.61	100.06	100.58	100.95	101.36	99.00	99.15
Formula 32(O)										
Si	–	–	0.002	–	–	–	0.056	0.007	0.006	0.00
Ti	0.020	0.014	0.117	0.023	0.030	–	0.321	0.011	0.042	0.022
Al	16.134	15.975	15.886	16.153	15.881	16.018	16.194	15.570	15.774	15.364
Cr	–	–	0.016	–	–	–	–	0.028	0.049	–
Fe^{3+}	0.000	0.000	0.000	0.000	0.078	0.000	0.000	0.412	0.000	0.779
Fe^{2+}	6.380	6.359	6.285	6.645	6.253	6.196	6.630	6.157	3.868	5.846
Mn	–	0.168	0.064	0.009	0.224	0.100	0.272	0.041	0.027	0.093
Mg	1.344	1.421	1.529	1.072	1.440	1.524	0.026	1.934	4.276	2.075
Zn	0.020	0.062	0.030	–	0.122	0.152	0.012	0.023	–	0.116
Ca	0.015	–	–	–	–	–	–	–	–	–
Total (cations)	23.913	23.999	23.929	23.901	24.029	23.991	23.526	24.183	24.041	24.296
ΣR^{2+}	7.759	8.010	7.907	7.726	8.040	7.973	6.956	8.155	8.171	8.131
ΣR^{3+}	16.154	15.989	16.022	16.175	15.989	16.018	16.571	16.028	15.870	16.165
Atomic (%)										
Spinel	17.3	17.7	19.3	22.5	13.9	19.1	0.4	23.9	52.5	26.2
Hercynite	82.2	79.4	79.5	77.5	86.1	80.3	99.6	76.1	47.5	73.8

Abbreviations: na = not analyzed; nd = not detected
Fe^{2+} and Fe^{3+} were recalculated from total FeO after the method of Droop (1987).
$\Sigma R^{2+} = Fe^{2+}+Mn+Mg+Zn+Ca$. $\Sigma R^{3+} = Ti+Al+Cr+Fe^{3+}$.
[a]*Khamloet et al. (2014)*
[b]*Sutherland et al. (1998b)*
[c]*Sutherland et al. (1998a)*

sapphires from Pailin in Cambodia or from New England in Australia, but nearly the same as those from Kanchanaburi in Thailand (see also table 6).

Ilmenite ($FeTiO_3$) was found in only two samples from Di Linh and one sample from Dak Nong. These inclusions were black, opaque, and euhedral (figure 11B), and their identity was confirmed by Raman spectroscopic identification. A previous study, based on SEM-EDS analysis, also recognized ilmenite in sapphires from Di Linh and Binh Thuan (Smith et al., 1995). The chemical composition of the ilmenite inclusions in this study clearly belonged to the titanohematite series (ilmenite-hematite, $Il_{54-49}He_{40-34}$) (table 7). The low Mn content (<0.15 wt.% MnO) of these titanohematites was closer to that from an igneous magma source (Lindsley, 1991) as reported from Sybille Monzosyenite (Fuhrman et al., 1988), and different from ilmenite with higher Mn originating from metamorphic rocks from Western Australia (Cassidy et al., 1988). Moreover, their Mn contents

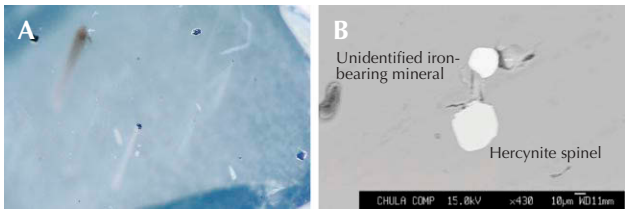

Figure 12. A: Several tiny unidentified iron-bearing minerals with cubic shape, shown in darkfield illumination. Photomicrograph by Doan Thi Anh Vu; magnified 50×. B: Backscattered electron image of unidentified cubic iron oxides and euhedral hercynite-spinel.

were similar to those of ilmenite in New England sapphires originating from silicate melt (Sutherland et al., 1998a) and different from those of ilmenite in Kanchanaburi sapphires from melt involved by subsequent contact metamorphism (Khamloet et al., 2014) (table 7).

Unidentified iron-bearing minerals were also observed in these sapphire samples. They presented as tiny black cubic crystals (less than 10 µm and a few around 30 µm) (figure 12A) with morphological forms similar to those identified for spinel inclusions. They were commonly associated with spinel inclusions and sometimes formed as composite inclusions (figure 12B). These iron-rich minerals contained up to 96% FeO and had aluminum contents ranging from 0.1 to 13% Al_2O_3 (table 8) and their Raman spectra indicated the presence of magnetite, with characteristic bands at 663 to 652 cm^{-1} (Faria et al., 1997). However, their atomic proportions, based on stoichiometric calculation as suggested by Droop (1987), yielded a $\Sigma R^{3+}/\Sigma R^{2+}$ ratio of almost 1:1, particularly Fe^{3+}/Fe^{2+} (see table 8), which was inconsistent with the formula of magnetite (Fe_3O_4), with an Fe^{3+}/Fe^{2+} ratio of 2:1. More details of these inclusions need to be worked out in the future.

Figure 13. A red cubic pyrochlore inclusion displaying halo and radial cracks in darkfield illumination. Photomicrograph by Doan Thi Anh Vu; magnified 50×.

TABLE 7. Representative EPMA analyses of ilmenite inclusions in sapphires from southern Vietnam, Thailand, and Australia.

Mineral phase analysis (wt.%)	Southern Vietnam			Thailand	Australia
	Dak Nong	Di Linh		Kanchanaburi[a]	New England[b]
	DN39	DL23	DL85		
SiO_2	0.11	0.10	nd	0.00	0.70
TiO_2	34.94	37.08	33.77	45.73	59.04
Al_2O_3	0.02	1.50	0.58	6.90	0.45
Cr_2O_3	nd	0.04	0.12	na	0.00
FeO_{total}	61.43	61.58	63.48	27.64	32.05
MnO	0.14	0.06	0.05	17.59	0.40
MgO	nd	0.18	0.64	0.98	1.85
ZnO	0.80	nd	nd	na	0.00
CaO	nd	0.01	nd	0.00	0.00
NiO	0.02	nd	0.03	na	na
Total (oxides)	97.46	100.54	98.67	98.84	94.57
Formula 3(O)					
Si	0.003	0.003	–	0.000	0.017
Ti	0.752	0.757	0.718	0.857	1.102
Al	0.001	0.048	0.019	0.202	0.013
Cr	–	0.001	0.003	–	0.000
Fe^{3+}	0.655	0.584	0.715	0.124	0.000
Fe^{2+}	0.814	0.814	0.786	0.452	1.330
Mn	0.003	0.001	0.001	0.371	0.008
Mg	–	0.007	0.027	0.036	0.068
Zn	0.017	–	–	–	0.000
Ca	–	0.000	–	0.000	0.000
Ni	0.000	–	0.001	–	–
Total (cations)	2.245	2.216	2.271	2.042	1.874
ΣR^{2+}	0.835	0.823	0.815	0.859	0.742
ΣR^{2+}	1.410	1.393	1.455	1.183	1.132
Atomic (%)					
Ilmenite	53.1	54.5	49.4	56.7	98.8
Magnetite	6.8	6.9	8.3	0.0	0.0
Hematite	38.7	33.7	39.8	29.9	0.0

Abbreviations: na = not analyzed; nd = not detected
Fe^{2+} and Fe^{3+} were recalculated from total FeO after the method of Droop (1987).
$\Sigma R^{2+} = Fe^{2+}+Mn+Mg+Zn+Ca+Ni$; $\Sigma R^{3+} = Ti+Al+Cr+Fe^{3+}$.
[a]Khamloet et al. (2014)
[b]Sutherland et al. (1998a)

TABLE 8. Representative EPMA analyses of unidentified iron-rich inclusions in sapphires from southern Vietnam.

Mineral phase analysis (wt.%)	Dak Nong		Di Linh		Krong Nang		Binh Thuan	
	DN73	DN89	DL14	DL50	KN05	KN19	PT17	PT18
SiO_2	0.33	0.02	nd	0.02	1.58	0.06	0.27	0.34
TiO_2	4.43	1.57	1.53	2.33	6.62	1.24	0.22	0.52
Al_2O_3	12.51	8.78	6.66	0.21	10.82	11.84	0.12	10.14
Cr_2O_3	0.18	nd	0.04	0.02	0.33	0.03	0.03	0.06
FeO_{total}	77.55	87.90	89.29	96.45	75.75	86.30	95.46	86.45
MnO	nd	0.14	1.49	0.41	0.08	0.18	1.81	1.57
MgO	0.98	0.18	0.29	1.36	0.15	0.37	0.88	0.05
ZnO	0.43	0.33	0.36	nd	0.31	0.51	nd	nd
CaO	0.12	nd	nd	nd	0.12	nd	nd	nd
NiO	0.02	nd	nd	0.03	0.10	nd	nd	nd
Total (oxides)	96.54	98.92	99.66	100.84	95.86	100.52	98.78	99.13
Formula 32(O)								
Si	0.110	0.001	–	0.008	0.523	0.020	0.104	0.116
Ti	1.106	0.051	0.405	0.645	1.648	0.310	0.063	0.133
Al	4.892	3.598	2.769	0.091	4.218	4.641	0.053	4.104
Cr	0.047	–	0.011	0.006	0.086	0.008	0.010	0.016
Fe^{3+}	9.753	12.429	13.148	14.925	8.501	11.658	15.700	12.266
Fe^{2+}	11.769	13.121	13.183	14.740	12.460	12.349	14.788	12.571
Mn	–	0.041	0.446	0.128	0.023	0.051	0.585	0.457
Mg	0.485	0.092	0.150	0.748	0.073	0.183	0.498	0.026
Zn	0.105	0.085	0.095	–	0.075	0.125	–	–
Ca	0.043	–	–	–	0.041	–	–	–
Ni	0.005	–	–	0.008	0.027	–	–	–
Total (cations)	28.315	29.784	30.206	31.299	27.676	29.345	31.801	29.690
ΣR^{2+}	12.407	13.339	13.874	15.624	12.699	12.708	15.871	13.054
ΣR^{3+}	15.908	16.078	16.333	15.667	14.453	16.617	15.826	16.519

Abbreviation: nd = not detected
Fe^{2+} and Fe^{3+} were recalculated from total FeO after the method of Droop (1987).
$\sum R^{2+} = Fe^{2+}+Mn+Mg+Zn+Ca+Ni$. $\sum R^{3+} = Ti+Al+Cr+Fe^{3+}$.

Pyrochlore was recognized as an inclusion in three sapphire samples from Dak Nong and a couple of samples from Krong Nang. They formed similarly red cubic crystals, which were commonly surrounded by radial cracks (figure 13). Based on SEM-EDS analysis, Smith et al. (1995) previously reported uranpyrochlore, $(Ca,U)_2(Ti, Nb, Ta)_2O_6$, in sapphires from Di Linh and Binh Thuan. EPMA analyses of pyrochlore in this study yielded a high U content (about 19–22% in ΣR^{2+}), a high Nb content leading to a Nb/Ta ratio ≥ 8, and a (Nb+Ta)/Ti ratio of about 2 (table 9), all within the compositional range of uranpyrochlore (Hogarth, 1977). These compositions were similar to those found in Australian sapphires from Anakie (Guo et al., 1996) and New England (Sutherland et al., 1998a).

DISCUSSION

It has been suggested that sapphire and ruby deposited within basaltic terranes could not have crystallized directly from basaltic magma (Coenraads, 1992; Levinson and Cook, 1994; Guo et al., 1996; Sutherland et al., 1998a, 2002, 2015; Khamloet et al., 2014; Promwongnan and Sutthirat, 2019). A corroded surface is a typical feature observed in basalt-associated sapphires, clearly indicating transport by the hot magma. This has also been reported for sapphires from Di Linh and Binh Thuan (Smith et al., 1995). A petrochemical study of sapphire-associated basalts from Dak Nong has also suggested that these xenocrystic sapphires may have formed in the boundary between the lower crust and upper mantle prior to corrosive transport in alkali basaltic magma

TABLE 9. Representative EPMA analyses of pyrochlore inclusions found in sapphires from southern Vietnam and Australia.

Mineral phase analysis (wt.%)	Southern Vietnam				Australia	
	Dak Nong		Krong Nang		Anakie[a]	New England[b]
	DN35	DN77	KN18	KN36		
SiO_2	0.23	0.37	0.55	0.33	na	0.00
TiO_2	11.67	11.20	10.59	11.63	11.48	10.14
FeO	1.68	1.38	1.54	1.57	1.51	0.30
MnO	0.37	0.19	0.08	0.03	na	na
CaO	6.86	6.63	6.26	6.89	5.58	5.49
Na_2O	4.33	5.11	4.44	5.24	4.27	5.92
K_2O	0.04	0.05	0.06	0.09	na	na
Nb_2O_5	33.61	32.24	33.88	33.03	32.99	38.48
Ta_2O_5	6.05	6.50	5.97	6.34	6.58	4.44
ThO_2	7.88	7.31	7.00	7.61	8.56	1.99
UO_2	22.28	23.06	23.83	22.32	21.80	30.88
ZrO_2	0.08	0.15	0.01	0.02	0.20	na
Y_2O_3	nd	0.08	0.12	0.08	0.66	na
Ce_2O_3	0.12	0.35	0.34	0.28	0.48	na
Nd_2O_3	0.14	0.17	nd	0.06	0.54	na
Total (oxides)	95.36	94.40	94.67	95.51	94.90	97.64
Formula 6(O)						
Si	0.016	0.026	0.039	0.023	–	0.000
Ti	0.605	0.591	0.557	0.601	0.607	0.518
Fe	0.097	0.081	0.090	0.090	0.089	0.017
Mn	0.022	0.011	0.005	0.002	–	–
Ca	0.506	0.498	0.469	0.508	0.420	0.400
Na	0.578	0.643	0.601	0.698	0.582	0.780
K	0.003	0.004	0.005	0.008	–	–
Nb	1.046	1.022	1.070	1.026	1.048	1.182
Ta	0.113	0.124	0.113	0.118	0.126	0.082
Th	0.123	0.117	0.111	0.119	0.137	0.031
U	0.341	0.360	0.370	0.341	0.341	0.467
Zr	0.003	0.005	0.000	0.001	0.007	0.000
Y	–	0.003	0.005	0.003	0.025	–
Ce	0.003	0.009	0.009	0.007	0.012	–
Nd	0.000	0.000	–	0.000	0.014	–
Total (cations)	3.460	3.498	3.444	3.546	3.411	3.477
ΣR^{2+}	1.674	1.719	1.651	1.767	1.628	1.694
Nb/Ta	9	8	9	9	8	14
(Nb+Ta)/Ti	2	2	2	2	2	2
$U/\Sigma R^{2+}$	20	21	22	19	21	28

Abbreviation: na = not analyzed; nd = not detected
ΣR^{2+} = Fe+Mn+Ca+Na+K+Th+U+Zr+Y+Ce+Nd
[a]*Guo et al. (1996)*
[b]*Sutherland et al. (1998a)*

(Garnier et al., 2005). Moreover, a hypothesis has recently been proposed that the original crystallization of alluvial Dak Nong sapphires would have taken place in the shallow crust within an iron-rich syenite melt in collaboration with carbonate-H_2O-CO_2 fluid phases, based on the geochemistry of syngenetic mineral inclusions (i.e., zircon, columbite, oligoclase, and Al-Ti-hematite) (Izokh et al., 2010).

Based on the results of this detailed study, the most common syngenetic mineral inclusions (ferrocolumbite, alkali feldspar, and zircon) were similar in composition to those in Dak Nong sapphires (Izokh et al., 2010) as well as alkaline felsic inclusion groups in other alluvial basalt-related sapphires (Guo et al., 1996). Although hercynite spinel and ilmenite (titanohematite) inclusions observed in this study were quite different from Al-Ti-hematite in Dak Nong sapphires (containing 85.6 wt.% Fe_2O_3, 11.9 wt.% Al_2O_3, and 1.57 wt.% TiO_2 as reported by Izokh et al., 2010), they still favored igneous sources instead of metamorphic sources. Although columbite and pyrochlore in the studied sapphires were chemically close to the inclusions Guo et al. (1996) proposed as representing a carbonatite assemblage, they were also similar to those found in alluvial basalt-associated sapphires from silicate melt origin (Sutherland et al., 1998a). Therefore, both columbite and pyrochlore may relate to silicate melts to indicate the original source of these sapphires.

Consequently, a unique mineral inclusion suite including alkali feldspar, zircon, hercynitic spinel, and ilmenite appears to have crystallized from alkaline felsic magma, which is relevant to the original source of sapphires from southern Vietnam. This magmatism should have taken place extensively prior to fractionated crystallization in the lower crust. This model agrees well with the genetic model proposed by Aspen et al. (1990), Sutherland et al. (1998a, 2009), Pin et al. (2006), Zaw et al. (2006), Upton et al. (2009), Khamloet et al. (2014), and Promwongnan and Sutthirat (2019).

Based on the geological setting in southern Vietnam, granite and granosyenite occurred in the Triassic and Cretaceous during orogenic periods due to Indosinian-Yangtze (South China) collision and Paleo-Pacific plate subduction, respectively (Carter et al., 2001; Nguyen et al., 2004; Tri and Khuc, 2011; Shellnutt et al., 2013). Subsequently, alkali basaltic magmas in southern Vietnam had probably been derived from garnet peridotite of the asthenosphere at high pressure (<4 GPa) and high temperature (about 1470°C) (Hoang and Flower, 1998), and mixed with recycling oceanic crustal materials from Paleo-Pa-

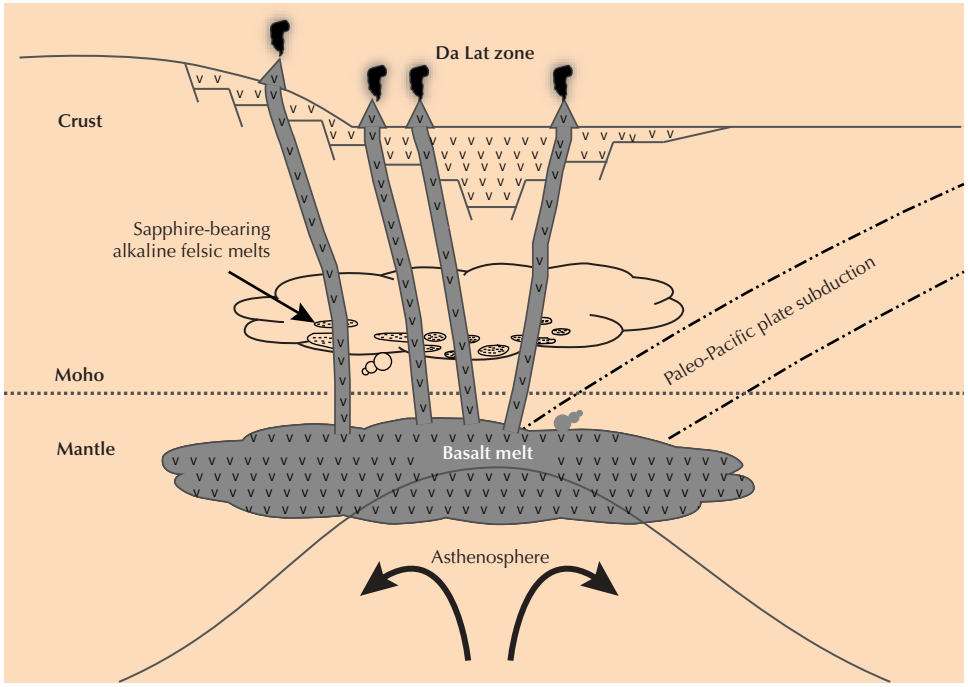

Figure 14. This illustration shows an alkaline felsic melt as the environment for sapphire origin, based on the alkali basalt and crustal evolution models for southern Vietnam (Hoang and Flower, 1998; Tri and Khuc, 2011; Anh et al., 2018).

cific plates that subducted beneath the Southeast Asian continental margin (Anh et al., 2018) during the early Tertiary Indian-Eurasian collision. Rising penetration at close to the Moho, an unconformity zone boundary between lower continental crust and upper mantle, located at about 32–75 km depth (Teng et al., 2013), the heat and volatility separated from these alkaline mafic melts caused the extensive melting of silicate rocks (granite and granosyenite) at lower-crust level with the formation of alkaline felsic melt (figure 14). Sapphires should have crystallized directly during the slow cooling of this alkaline felsic melt. Afterwards, the alkali basaltic magma from the asthenosphere of mantle rose and then brought these sapphires onto the surface via volcanic eruption.

CONCLUSIONS

Mineral inclusions including ferrocolumbite, zircon, alkali feldspar, hercynite spinel, ilmenite (titanohematite), and pyrochlore were identified in sapphires from the main deposits in southern Vietnam. On the basis of chemical composition, they can be mostly grouped into alkaline felsic suites. An alkaline felsic melt is proposed as the crystallization environment for the original formation of these sapphires. Detailed studies on U/Pb dating and trace analysis of zircon inclusions should be carried out to support time scale and original formation of the sapphire hosts. Moreover, unidentified iron-bearing inclusions may give more significant information related to the crystallization environment.

ABOUT THE AUTHORS

Mrs. Vu is a doctor's degree student in geology at Chulalongkorn University in Bangkok and a lecturer at the Faculty of Geology, University of Science, Vietnam National University in Ho Chi Minh City. Dr. Salam and Dr. Fanka are lecturers at the Geology Department, Faculty of Science, Chulalongkorn University. Dr. Belousova is a research fellow at the Department of Earth and Planetary Science, Macquarie University in Sydney. Dr. Sutthirat (chakkaphan.s@chula.ac.th) is a professor of earth sciences at the Geology Department, Faculty of Science, Chulalongkorn University and an academic advisor to the Gem Testing Laboratory of the Gem and Jewelry Institute of Thailand (GIT).

ACKNOWLEDGMENTS

The authors would like to thank all staff members of the Geology Department, Faculty of Science, Chulalongkorn University, for their support in sample preparation and analyses. This research is a part of PhD thesis of the first author who has been supported by the Scholarship Program for ASIAN Countries of Chulalongkorn University.

REFERENCES

Anh H.T.H., Choi S.H., Yu Y., Hieu P.T., Hoang N.K., Ryu J. (2018) Geochemical constraints on the spatial distribution of recycled oceanic crust in the mantle source of late Cenozoic basalts, Vietnam. *Lithos*, Vol. 296, pp. 382–395, http://dx.doi.org/10.1016/j.lithos.2017.11.020

Aspen P., Upton B.G.J., Dicken A.P. (1990) Anorthoclase, sanidine and associated megacrysts in Scottish alkali basalts: High pressure syenitic debris from upper mantle sources? *European Journal of Mineralogy*, Vol. 2, pp. 503–517, http://dx.doi.org/10.1127/ejm/2/4/0503

Barr S., MacDonald A. (1981) Geochemistry and geochronology of late Cenozoic basalts of Southeast Asia: Summary. *Geological Society of America Bulletin*, Vol. 92, No. 8, pp. 1069–1142, http://dx.doi.org/10.1130/0016-7606(1981)92%3C508:GAGOLC%3E2.0.CO;2

Belousova E., Griffin W., O'Reilly S., Fisher N. (2002) Igneous zircon: Trace element composition as an indicator of source rock type. *Contributions to Mineralogy and Petrology*, Vol. 143, No. 5, pp. 602–622, http://dx.doi.org/10.1007/s00410-002-0364-7

Carter A., Roques D., Bristow C., Kinny P. (2001) Understanding Mesozoic accretion in Southeast Asia: Significance of Triassic thermotectonism (Indosinian orogeny) in Vietnam. *Geology*, Vol. 29, No. 3, pp. 211–214, http://dx.doi.org/10.1130/0091-7613(2001)029

Cassidy K., Groves D.I., Binns R.A. (1988) Manganoan ilmenite formed during regional metamorphism of Archean mafic and ultramafic rocks from Western Australia. *Canadian Mineralogist*, Vol. 26, pp. 999–1012.

Cerný P., Ercit T.S. (1985) Some recent advances in the mineralogy and geochemistry of Nb and Ta in rare-element granitic pegmatites. *Bulletin de Minéralogie*, Vol. 108, pp. 499–532, http://dx.doi.org/10.3406/bulmi.1985.7846

Coenraads R. (1992) Sapphires and rubies associated with volcanic provinces: Inclusions and surface features shed light on their origin. *Australian Gemmologist*, Vol. 18, No. 3, pp. 70–78.

Deer W.A., Howie R.A., Zussman J. (2013) *An Introduction to the Rock-Forming Minerals*. Longman, Essex, UK, 696 pp.

Droop G.T.R. (1987) A general equation for estimating Fe^{3+} concentrations in ferromagnesian silicates and oxides from microprobe analyses, using stoichiometric criteria. *Mineralogical Magazine*, Vol. 51, No. 361, pp. 431–435, http://dx.doi.org/10.1180/MINMAG.1987.051.361.10

Faria D.L.A., Silva S.V., Oliveira M.T.M. (1997) Raman microspectroscopy of some iron oxides and oxyhydroxides. *Journal of Raman Spectroscopy*, Vol. 28, No. 11, pp. 873–878, http://dx.doi.org/10.1002/(SICI)1097-4555(199711)28:11%3C873:AID-JRS177%3E3.0.CO;2-B

Fuhrman M., Frost B.R., Lindsley D.H. (1988) Crystallization conditions of the Sybille Monzosyenite, Laramie Anorthosite Complex, Wyoming. *Journal of Petrology*, Vol. 29, No. 3, pp. 699–729, http://dx.doi.org/10.1093/petrology/29.3.699

Garnier V., Ohnenstetter D., Giuliani G., Fallick A.E., Trinh P., Quang V., Van L., Schwarz D. (2005) Basalt petrology, zircon ages and sapphire genesis from Dak Nong, southern Vietnam. *Mineralogical Magazine*, Vol. 69, No. 1, pp. 21–38, http://dx.doi.org/10.1180/0026461056910233

Guo J., O'Reilly S.Y., Griffin W.L. (1996) Corundum from basaltic terrains: A mineral inclusion approach to the enigma. *Contributions to Mineralogy and Petrology*, Vol. 122, No. 4, pp. 368–386, http://dx.doi.org/10.1007/s004100050134

Hoa T.T., Phuong N.T., Anh T.T., Van V.V., Y N.V., Hoang N., Thanh H.H., Anh P.L., Nien B.A., Hung T.Q., Dung P.T., Lam T.H., Hang H.V., Anh T.V., Chuong V.D., Hung P.V., Quan V.M. and eds. (2005) Study of forming conditions and distribution laws of precious and rare minerals related to magmatic activity in Central Vietnam and Tay Nguyen Highlands. *State-level Project, code DTDL-2003/07*, Vol. I, pp. 347 (in Vietnamese).

Hoang N., Flower M. (1998) Petrogenesis of Cenozoic basalts from Vietnam: Implication for origins of a 'diffuse igneous province'. *Journal of Petrology*, Vol. 39, No. 3, pp. 369–395, http://dx.doi.org/10.1093/petroj/39.3.369

Hoang T.H.A., Choi S.H., Yu Y., Pham T.H., Nguyen K.H., Ryu Y. (2018) Geochemical constraints on the spatial distribution of recycled oceanic crust in the mantle source of late Cenozoic basalts, Vietnam. *Lithos*, Vol. 296-299, pp. 382–395, http://dx.doi.org/10.1016/j.lithos.2017.11.020

Hogarth D.D. (1977) Classification and nomenclature of the pyrochlore group. *American Mineralogist*, Vol. 62, No. 5-6, pp. 403–410.

Huong L.T.T., Vuong B.T.S., Khoi N.N., Satitkune S., Wanthanachaisaeng B., Hofmeister W., Häger T., Hauzenberger C. (2016) Geology, gemmological properties and preliminary heat treatment of gem-quality zircon from the Central Highlands of Vietnam. *Journal of Gemmology*, Vol. 35, No. 4, pp. 308–318, http://dx.doi.org/10.15506/JOG.2016.35.4.308

Hutchison C.S. (1989) *Geological Evolution of South-east Asia*. Clarendon Press, Oxford, UK.

Izokh A.E., Smirnov S.Z., Egorova V.V., Anh T.T., Kovyazin S.V., Phuong N.T., Kalinina V.V. (2010) The conditions of formation of sapphire and zircon in the areas of alkali-basaltoid volcanism in Central Vietnam. *Russian Geology and Geophysics*, Vol. 51, No. 7, pp. 719–733, http://dx.doi.org/10.1016/j.rgg.2010.06.001

Khamloet P., Pisutha-Arnond V., Sutthirat, C. (2014) Mineral inclusions in sapphire from the basalt-related deposit in Bo Phloi, Kanchanaburi, western Thailand: Indication of their genesis. *Russian Geology and Geophysics*, Vol. 55, No. 9, pp. 1087–1102, http://dx.doi.org/10.1016/j.rgg.2014.08.004

Lee T., Lo C.H., Chung S.L., Chen C.Y., Wang P.L., Lin W.P., Hoang N., Chi C., Yem N. (1998) $^{40}Ar/^{39}Ar$ Dating Result of Neogene Basalts in Vietnam and its Tectonic Implication. *Mantle Geodynamics and Plate Interactions in East Asia*, *AGU Monograph*, Vol. 27, pp. 317–330, http://dx.doi.org/10.1029/GD027p0317

Lepvrier C., Vuong N.V., Maluski H., Thi P.T., Vu T.V. (2008) Indosinian tectonics in Vietnam. *Comptes Rendus Geoscience*, Vol. 340, No. 2, pp. 94–111, http://dx.doi.org/10.1016/j.crte.2007.10.005

Levinson A.A., Cook F.A. (1994) Gem corundum in alkali basalt: Origin and occurrence. *G&G*, Vol. 30, No. 4, pp. 253–262, http://dx.doi.org/10.5741/GEMS.30.4.253

Lindsley D.H. (1991) Experimental studies of oxide minerals. In D.H. Lindsley, Ed., *Oxide Minerals: Petrologic and Magnetic Significance. Reviews in Mineralogy*, Vol. 25, Mineralogical Society of America, pp. 69–106.

Long P.V., Vinh H., Garnier V., Giuliani G., Ohnenstetter D., Lhomme T., Schwarz D., Fallick A.E., Dubessy J., Trinh P.T. (2004) Gem corundum deposits in Vietnam. *Journal of Gemmology*, Vol. 29, No. 3, pp. 129–147, http://dx.doi.org/10.15506/JOG.2004.29.3.129

Mackay D., Simandl G. (2015) Pyrochlore and columbite-tantalite as indicator minerals for specialty metal deposits. *Geochemistry: Exploration, Environment, Analysis*, Vol. 15, No. 2-3, pp. 167–178, http://dx.doi.org/10.1144/geochem2014-289

Metcalfe I. (1988) Origin and assembly of South-east Asian continental terranes. *Geological Society, London, Special Publications*, Vol. 37, No. 1, pp. 101–118, http://dx.doi.org/10.1144/GSL.SP.1988.037.01.08

——— (1996) Pre-Cretaceous evolution of SE Asian terranes. *Geological Society, London, Special Publications*, Vol. 106, No. 1, pp. 97–122, http://dx.doi.org/10.1144/GSL.SP.1996.106.01.09

——— (2009) Late Palaeozoic and Mesozoic tectonic and palaeogeographical evolution of SE Asia. In E. Buffetaut, G. Cuny, J. Le Loeuff, and V. Suteethorn, Eds., *Late Palaeozoic and Mesozoic Ecosystems in SE Asia*. The Geological Society of London, Special Publication, Vol. 315, No. 1, pp. 7–23.

——— (2011) Palaeozoic-Mesozoic history of SE Asia. *Geological Society of London Special Publications*, Vol. 355, No. 1, pp. 7–35, http://dx.doi.org/10.1144/SP355.2

Nguyen T., Satir M., Siebel W., Chen F. (2004) Granitoids in the Dalat zone, southern Vietnam: Age constraints on magmatism and regional geological implications. *International Journal of Earth Sciences*, Vol. 93, No. 3, pp. 329–340, http://dx.doi.org/10.1007/s00531-004-0387-6

Palke A.C., Saeseaw S., Renfro N.D., Sun Z., McClure S. (2019) Geographic origin determination of blue sapphire. *G&G*, Vol. 55, No. 4, pp. 536–579, http://dx.doi.org/10.5741/gems.55.4.536

Pin C., Monchoux P., Paquette J.L., Azambre B., Wang P.C., Martin R.F. (2006) Igneous albititic dikes in orogenic lherzolites, Western Pyrenees, France: A possible source for corundum and alkali feldspar xenocrysts in basalt terranes. II. Geochemical and petrogenetic considerations. *Canadian Mineralogist*, Vol. 44, No. 4, pp. 817–842, http://dx.doi.org/10.2113/gscanmin.44.4.817

Promwongnan S., Sutthirat C. (2019) Mineral inclusions in ruby and sapphire from the Bo Welu gem deposit in Chanthaburi, Thailand. *G&G*, Vol. 55, No. 3, pp. 354–369, http://dx.doi.org/10.5741/GEMS.55.3.354

Rangin C., Huchon P., Le Pichon X., Bellon H., Lepvrier C., Roques D., Hoe N.D., Quynh P.V. (1995) Cenozoic deformation of central and south Vietnam. *Tectonophysics*, Vol. 251, No. 1-4, pp. 180–196, http://dx.doi.org/10.1016/0040-1951(95)00006-2

Rubatto D., Gebauer D. (2000) Use of cathodoluminescence for U-Pb zircon dating by ion microprobe: Some examples from the Western Alps. In M. Pagel et al., Eds., *Cathodoluminescence in Geosciences*, Springer, Berlin, pp. 373–400.

Saminpanya S., Sutherland F. (2011) Different origins of Thai area sapphire and ruby, derived from mineral inclusions and co-existing minerals. *European Journal of Mineralogy*, Vol. 23, No. 4, pp. 683–694, http://dx.doi.org/10.1127/0935-1221/2011/0023-2123

Sengör A.M.C., Altiuner D., Cin A., Ustaömer T., Hsü K.J. (1988) Origin and assembly of the Tethyan orogenic collage at the expense of Gondwana land. In M.G. Audley-Chalerles and A. Hallam, Eds., Gondwana and Tethys. *The Geological Society of London, Special Publication*, Vol. 37, No. 1, pp. 119–181, http://dx.doi.org/10.1144/GSL.SP.1988.037.01.09

Shellnutt J., Lan C.-Y., Long T., Usuki T., Yang H.-J., Mertzman S., Iizuka Y., Chung S.-L., Wang K.-L., Hsu W.-Y. (2013) Formation of Cretaceous Cordilleran and post-orogenic granites and their microgranular enclaves from the Dalat zone, southern Vietnam: Tectonic implications for the evolution of Southeast Asia. *Lithos*, Vol. s 182–183, pp. 229–241, http://dx.doi.org/10.1016/j.lithos.2013.09.016

Smith C.P., Kammerling R.C., Keller A.S., Peretti A., Scarratt K.V., Khoa N.D., Repetto S. (1995) Sapphires from southern Vietnam. *G&G*, Vol. 31, No. 3, pp. 168–186, http://dx.doi.org/10.5741/GEMS.31.3.168

Sutherland F., Hoskin P., Fanning C., Coenraads R. (1998a) Models of corundum origin from alkali basaltic terrains: A reappraisal. *Contributions to Mineralogy and Petrology*, Vol. 133, No. 4, pp. 356–372, http://dx.doi.org/10.1007/s004100050458

Sutherland F., Schwarz D., Jobbins E.A., Coenraads R., Webb G. (1998b) Distinctive gem corundum suites from discrete basalt fields: A comparative study of Barrington, Australia and West Pailin, Cambodia, Gemfields. *Journal of Gemmology*, Vol. 26, No. 2, pp. 65–85.

Sutherland F., Bosshart G., Fanning C., Hoskin P.W.O., Coenraads R. (2002) Sapphire crystallization, age and origin, Ban Huai Sai, Laos: Age based on zircon inclusions. *Journal of Asian Earth Sciences*, Vol. 20, No. 7, pp. 841–849, http://dx.doi.org/10.1016/S1367-9120(01)00067-0

Sutherland F.L., Zaw K., Meffre S., Giuliani G., Fallick A.E., Graham L., Webb G.B. (2009) Gem-corundum megacrysts from east Australian basalt fields: Trace elements, oxygen isotopes and origins. *Australian Journal of Earth Sciences*, Vol. 56, No. 7, pp. 1003–1022, http://dx.doi.org/10.1080/08120090903112109

Sutherland F.L., Piilonen P.C., Zaw K., Meffre S., Thompson J. (2015) Sapphire within zircon-rich gem deposits, Bo Loei, Ratanakiri Province, Cambodia: Trace elements, inclusions, U–Pb dating and genesis. *Australian Journal of Earth Sciences*, Vol. 62, No. 6, pp. 761–773.

Teng J., Zhang Z., Zhang Y., Pi J., Deng Y., Zhang X., Wang C.-Y., Gao R., Liu C. (2013) Moho depth, seismicity and seismogenic structure in China mainland. *Tectonophysics*, Vol. 627, pp. 108–121, http://dx.doi.org/10.1016/j.tecto.2013.11.008

Tri T.V., Khuc V. (2011) *Geology and Earth Resources of Vietnam*. General Department of Geology and Minerals of Vietnam, Ha Noi, Publishing House for Science and Technology, 634 pp.

Upton B.J.G., Finch A.A., Slaby E. (2009) Megacrysts and salic xenoliths in Scottish alkali basalts: Derivatives of deep crustal intrusions and small melt fractions from the upper mantle. *Mineralogical Magazine*, Vol. 73, No. 6, pp. 943–956, http://dx.doi.org/10.1180/minmag.2009.073.6.943

Vu D.T.A. (2010) Petrographical characteristics and genesis of corundum in Vietnam. University of Science, VNU-Ho Chi Minh City, 120 pp.

——— (2018) Gemological characteristics and the quality of sapphire from Krong H'Nang - Dak Lak. *Science and Technology Development Journal – Natural Sciences*, Vol. 1, No. T5, pp. 263–269, http://dx.doi.org/10.32508/stdjns.v1iT5.559

Williams I.S., Claesson S. (1987) Isotopic evidence for the Precambrian provenance and Caledonian metamorphism of high grade paragneisses from the Seve Nappes, Scandinavian Caledonides. *Contributions to Mineralogy and Petrology*, Vol. 97, No. 2, pp. 205–217, http://dx.doi.org/10.1007/bf00371240

Zaw K., Sutherland F.L., Dellapasqua F., Ryan C.G., Yui T., Mernagh T.P., Duncan D. (2006) Contrasts in gem corundum characteristics, eastern Australian basaltic fields: Trace elements, fluid/melt inclusions and oxygen isotopes. *Mineralogical Magazine* Vol. 70, No. 6, pp. 669–687, http://dx.doi.org/10.1180/0026461067060356